Rotor Blade Stability in Turbulent Flows—Part I

Y. K. Lin,* Y. Fujimori,† and S. T. Ariaratnam‡ *University of Illinois at Urbana-Champaign, Urbana, Ill.*

The effect of turbulence in the atmosphere on the motion stability of a helicopter blade is investigated. Modeling turbulence as a random field, statistically stationary in time and homogeneous in space, the method of stochastic average of Stratonovich is used to obtain equivalent Itô stochastic equations, from which the Fokker-Planck equation for the transition probability density and the equations for various stochastic moments can be derived. As an exploratory study, only flapping and torsional motions are considered; the results are reported in two parts. In Part I, the present paper, equations of motion are derived which are reducible to those obtained previously by Sissingh and Kuczynski when the turbulence terms are removed. The in-plane turbulence components appear in the coefficients of these equations; thus, they affect the stability of the flapping and torsional motions. On the other hand, the normal turbulence component appears in the inhomogeneous terms in the equations; its statistical properties, while affecting the level of system response, do not change a stable solution to an unstable solution. Then detailed discussions are given for the reduced case of uncoupled flapping in a hovering flight. This simple case is theoretically interesting, since closed-form solutions can be obtained and considerable insight can be gained from the analysis. Certain mathematical tools involving stochastic processes which may be foreign to engineers are explained in the Appendix. Solutions for the case of forward flights for both coupled and uncoupled motions are presented in Part II.

= lift curve slope а В = tip loss factor = blade chord cE[]= ensemble average F G $=(I_{\beta}/16I_{\alpha})(c/R)^{2}$ = flapping moment = generalized force for torsion h $=B^4\gamma/8$ = feathering mass moment of inertia of a blade = $\int_0^R i_\alpha dr (kg-m^2)$ = flapping mass moment of inertia of a blade, kg-m² I_{β} = polar mass moment of inertia about elastic axis per unit length of a blade, kg-m = unit lift = generalized mass for torsion M, = drift coefficients m_j = blade flapping frequency/blade angular velocity Q $=cI_{\beta}/(4RI_{\alpha})$ = unit torque q= transition probability density of response am q_A plitude R = rotor radius = distance from the center of the hub = nondimensional perpendicular velocity at the blade element U_T = nondimensional tangential velocity at the blade element U= lateral turbulence component, m/s

Nomenclature

Received July 6, 1978; revision received Jan. 3, 1979. Copyright © American Institute of Aeronautics and Astronautics, Inc., 1978. All rights reserved.

= longitudinal turbulence component, m/s

= forward flying velocity, m/s

Index categories: Propeller and Rotor Systems; Structural Dynamics; Structural Stability.

*Professor, Dept. of Aeronautical & Astronautical Engineering. Associate Fellow AIAA.

†Graduate Student; presently, Principal Research Officer, National Aerospace Laboratory, Tokyo, Japan. Member AIAA.

‡Visiting Professor from University of Waterloo, Ontario, Canada.

W	= total vertical flow velocity, in-flow plus vertical					
	turbulence component, m/s					
W_k	= Wiener process					
	=r/R					
Z_1, Z_2	= normalized turbulence velocities					
	= torsion angle					
	= flapping angle					
	$=R^4\rho ca/I_\beta$, blade lock number					
$\stackrel{\cdot}{\eta}$	$=V/\Omega R$					
	= blade pitch angle = $\theta_0 + x\alpha + \theta_s \sin \psi + \theta_c \cos \psi$					
	= collective pitch					
θ_c, θ_s	= cyclic pitch					
λ	$=W/\Omega R$					
μ	$=v/\Omega R$, advance ratio					
ξ	$=U/\Omega R$					
ρ	= air density					
σ_{ij}	= diffusion coefficients					
τ	= time lag					
Φ	= cosine spectrum					
Ψ	= sine spectrum					
ψ	$=\Omega t$, azimuth angle					
Ω	= blade angular velocity					
ω_{α}	= torsion frequency/ Ω					

Introduction

= derivative with respect to azimuth angle ψ

NLIKE the propeller of a fixed wing aircraft, the rotor blade system of a helicopter plays the roles of a lifting surface and control device, in addition to being a thrust generator. In many cases, the source of severe vibration can be traced to a poor blade system design. Therefore, it is essential to understand fully the dynamic behavior of rotor blades.

The studies of rotor blade dynamics began naturally from a deterministic approach in which turbulence in the surrounding flow was ignored. The simplest model was a centrally hinged rigid blade in uncoupled flapping motion. Further refinements included the considerations of multiblade systems, flapping-torsion and flapping-lagging couplings, blade elasticity, initial twist in the blade design, etc. (see, for example, Refs. 1-15). Without turbulence, the various rotor blade motions in forward flights are governed by differential

equations with periodically varying coefficients. Such equations are similar to the well-known Hill's equation in basic character, including the existence of instability regions, but the periodic coefficients in the rotor blade equations are so complicated that a closed-form solution for the instability regions is, in general, unattainable. A numerical procedure, consisting of computing the Floquet transition matrix and its eigenvalues has been used to determine the stability boundaries for such motions. 5,10,16

In a series of papers by Gaonkar, including some coauthored with Hohenemser and Yin, the vertical component of the turbulent flowfield was included in the analysis (see, for example, Refs. 17-19) and a similar problem was treated by Wan.²⁰ In these studies, the random turbulence terms appear only on the right-hand side of the differential equations, not as parametric excitations; consequently, they do not affect the system stability.

To the writers' knowledge, the effects of turbulence on the stability of rotor blade motion have not been dealt with in the literature. Therefore, the present investigation is directed toward revealing these effects.

Equation of Motion

In deriving the equations for flapping and torsional motions of a rotor blade, the same assumptions proposed in Refs. 4 and 8 will be made with regard to the structural and aerodynamic models. Briefly, they are as follows:

- A. Structural model
- 1) For the flapping motion, the blade is rigid, centrally hinged, with elastic restraint at the hinge.
- 2) For the torsional motion, the blade is elastic and the torsional angle varies spanwise linearly.
- 3) The mass and elastic centers coincide along the onequarter chord line.
 - B. Aerodynamic model
- 1) Flow is incompressible and sectionally two-dimensional; i.e., the spanwise flow is negligible.
- 2) The aerodynamic forces can be computed from the steady-state theory, except for the aerodynamic damping due to blade pitching for which the more accurate quasisteady theory should be used.
- 3) The lift slope is the same constant in the normal and reversed flows.
 - 4) Flow separation and stall do not occur.

In the normal flow region, the air approaches the blade from the leading edge; whereas, in the reversed flow region, it approaches from the trailing edge. These regions are depicted in Figs. 1a and 1b for the case $\mu < B$ and $\mu > B$, respectively. When $\mu > B$, a complete reversed flow region exists in the azimuth range $\pi + \epsilon < \psi < 2\pi - \epsilon$ which is labeled 3. Within $0 < \psi < \pi$, labeled 1, the flow is completely normal. In the remaining area, marked 2, both normal and reversed flows are present. The demarcation angle ϵ for regions 2 and 3 is computed from $\sin \epsilon = B/\mu$. When $\mu < B$, region 3 disappears altogether, and region 2 occupies the entire azimuth range $\pi < \psi < 2\pi$.

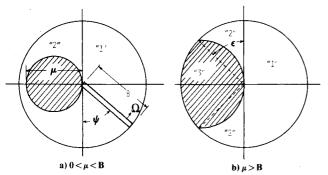


Fig. 1 Normal and reversed flow regions.

In the nomenclature used herein, the equations of motion for flapping and torsion may be written as follows:

$$I_{\beta}(\ddot{\beta} + p^2\beta) = F_{\beta}/\Omega^2 \tag{1}$$

$$M_t(\ddot{\alpha} + \omega_{\alpha}^2 \alpha) = G/\Omega^2$$
 (2)

where an overdot denotes one differentiation with respect to the azimuth angle $\psi = \Omega t$ (the nondimensional time). The flapping moment F_{β} is given by

$$F_{\beta} = \int r \mathrm{d}L = R^2 \int_0^1 x \ell \mathrm{d}x \tag{3}$$

For a linear torsion mode $\phi = x$, $0 \le x \le 1$, the generalized mass for torsion is:

$$M_t = \int_0^t x^2 i_\alpha d(Rx) = (1/3)Ri_\alpha = (1/3)I_\alpha$$
 (4)

and the generalized force

$$G = \int qx d(Rx) = R \int_0^1 qx dx$$
 (5)

The unit lift and torque, ℓ and q, depend on the flow velocity relative to the blade. At the blade section distant r from the hub center, the relative tangential and perpendicular velocities are:

$$\bar{U}_T = \Omega r + (v + V)\sin\psi + U\cos\psi$$

$$\bar{U}_P = W - [(v + V)\cos\psi - U\sin\psi]\beta - r\Omega\dot{\beta}$$

These can be divided by $R\Omega$ to yield the nondimensional velocities

$$U_T = x + (\mu + \eta)\sin\psi + \xi\cos\psi \tag{6}$$

$$U_P = \lambda - [(\mu + \eta)\cos\psi - \sin\psi]\beta - x\dot{\beta} \tag{7}$$

Note that $\lambda = W/R\Omega$ here is not usual in-flow ratio in a hypothetical nonturbulence environment, since W is the sum of the steady in-flow and the vertical velocity component of the random turbulence field.

From the steady aerodynamics.

$$\ell = \pm \left(\rho a c / 2\right) R^2 \Omega^2 \left(U_T^2 + U_P^2\right) \left[\theta + \left(U_P / U_T\right)\right] \tag{8}$$

where the plus and minus signs apply to the normal and reversed flow regions, respectively, and the total pitch angle θ is given by:

$$\theta = \theta_0 + x\alpha + \theta_s \sin\psi + \theta_c \cos\psi \tag{9}$$

In practice, $U_T \gg U_P$ and Eq. (8) may be simplified to

$$\ell = \pm (\rho a c / 2) R^2 \Omega^2 U_T^2 [\theta + (U_P / U_T)]$$
 (10)

The flapping moment F_{β} can be evaluated by substituting Eqs. (6, 7, 9, and 8) into Eq. (3).

To obtain the generalized force G for torsion, a quasisteady theory will be used. The blade pitching motion results in two lift components: one depends on the pitching velocity θ , the other depends on the pitching angle θ itself. In the normal flow region, the first component acts along the three-quarter chord line, whereas the second component acts along the one-quarter chord line. In the reversed flow region, the positions of the two components are also reversed.

Let the total unit torque q be separated into q_1 and q_3 according to the two lift components just mentioned; that is,

 q_1 depends on $\dot{\theta}$ and q_2 , on θ . Specifically,

$$q_I = -\left(\rho a c^3 / 16\right) \Omega^2 R U_T (x \dot{\alpha} + \dot{\theta}_r) \tag{11}$$

$$q_3 = (\rho a c^2 / 4) \Omega^2 R^2 U_T^2 (x \alpha + \theta_r + U_p / U_T)$$
 (12)

where $\theta_r = \theta_0 + \theta_s \sin \psi + \theta_c \cos \psi$, and following Ref. 8, the unsteady effect due to the time variation in U_P/U_T has been neglected. Since the elastic axis is assumed to coincide with the one-quarter chord line, q_I vanishes in the reversed flow and q_3 vanishes in the normal flow. Thus,

$$G = R \int_0^1 q_1 x dx$$
 in the normal flow (13a)

$$G = R \int_0^l q_3 x dx \text{ in the reversed flow}$$
 (13b)

Equations (6), (7), and (11-13) provide the complete information for the generalized force G for torsion. It is interesting to note that in the reversed flow region, the "aerodynamic spring constant" is negative, and the aerodynamic damping is zero. Therefore, a large torsional response can be expected when the advance ratio μ is high.

Having evaluated F_{β} and G, Eqs. (1) and (2) can now be rearranged, with those terms involving β and α and their derivatives moved to the left-hand sides. The remaining inhomogeneous terms on the right-hand sides of the equations do not affect the system stability; hence, they will be dropped from the ensuing discussion. After some algebraic work, the homogeneous parts of the two equations are cast in the following matrix form:

$$\begin{cases}
\ddot{\beta} \\
\ddot{\alpha}
\end{cases} + \frac{\gamma}{2} \begin{bmatrix}
\tilde{C} & 0 \\
6Q\tilde{\ell}_{r\dot{\beta}} & 6F\tilde{C}_{\alpha}
\end{bmatrix} \begin{cases}
\dot{\beta} \\
\dot{\alpha}
\end{cases} \\
+ \begin{bmatrix}
p^{2} + \frac{\gamma}{2}\tilde{K} & -\frac{\gamma}{2}\tilde{m}_{\alpha} \\
3\gamma Q\tilde{\ell}_{r\dot{\beta}} & \omega_{\alpha}^{2} + 3\gamma Q\tilde{K}_{\alpha}
\end{bmatrix} \begin{cases}
\beta \\
\alpha
\end{cases} = 0$$
(14)

The coefficients \tilde{C} , \tilde{K} ,... are periodic functions of the azimuth angle ψ , as well as functions of the nondimensional horizontal turbulence velocities $\xi(t)$ and $\eta(t)$. The vertical velocity $\lambda(t)$ appears only in the inhomogenous terms. Typically,

$$\tilde{K} = K + K_{\xi} \xi + K_{\eta} \eta + K_{\xi\xi} \xi^2 + K_{\eta\eta} \eta^2 + K_{\xi\eta} \xi \eta + \dots$$

where K, K_{ξ} ,... are now just periodic functions of ψ . Since turbulence velocities are expected to be small compared with the blade tip rotational speed $R\Omega$, it is reasonable to truncate the expressions for the coefficients at the linear terms in $\xi(t)$ and $\eta(t)$. Denoted by an overbar, the truncated versions of these coefficients can be grouped as:

$$\begin{pmatrix}
\bar{C} \\
\bar{K} \\
\bar{m}_{\alpha} \\
\bar{C}_{\alpha}
\end{pmatrix} = \begin{pmatrix}
C & C_{\xi} & C_{\eta} \\
K & K_{\xi} & K_{\eta} \\
m_{\alpha} & m_{\alpha\xi} & m_{\alpha\eta} \\
C_{\alpha} & C_{\alpha\xi} & C_{\alpha\eta} \\
K_{\alpha} & K_{\alpha\xi} & K_{\alpha\eta} \\
\ell_{r\beta} & \ell_{r\beta\xi} & \ell_{r\beta\eta} \\
\ell_{r\beta} & \ell_{r\beta\xi} & \ell_{r\beta\eta}
\end{pmatrix}$$
(15)

The elements of the 7×3 matrix on the right-hand side of Eq. (15) are given in Table 1. The expressions for these elements

are different for different flow regions, although they are periodic functions of ψ . For the first three rows, it is only necessary to distinguish regions 1, 2, and 3. For the remaining rows, the mixed flow region 2 must be further separated into 2_n and 2_r in which the normal flow and the reversed flow prevail, respectively.

Uncoupled Flapping Motion in Hovering Flight

Letting $\alpha = 0$ in the first row of Eq. (15), one obtains the equation for uncoupled flapping motion:

$$\ddot{\beta} + \frac{\gamma}{2} \, \bar{C} \dot{\beta} + \left(p^2 + \frac{\gamma}{2} \, \bar{K} \right) \beta = 0 \tag{16}$$

In a hovering flight, $\mu = 0$, the mixed and reversed flow regions no longer exist. Then Eq. (16) is simplified to:

$$\ddot{\beta} + [h + Z_1(t)]\dot{\beta} + [p^2 + Z_2(t)]\beta = 0$$
 (17)

where

$$Z_{I}(t) = (B^{3}\gamma/6)\left[\eta(t)\sin\psi + \xi(t)\cos\psi\right] \tag{18}$$

$$Z_2(t) = (B^3 \gamma/6) \left[\eta(t) \cos \psi - \xi(t) \sin \psi \right]$$

$$h = B^4 \gamma / 8 \tag{19}$$

It is seen that even when $\xi(t)$ and $\eta(t)$ are stationary§ random processes, $Z_1(t)$ and $Z_2(t)$ generally are nonstationary. However, if $\xi(t)$ and $\eta(t)$ are stationary, uncorrelated, and identically distributed, then it can be shown that $Z_1(t)$ and $Z_2(t)$ are also stationary. For such a case, the spectral densities and cross-spectral densities of $Z_1(t)$ and $Z_2(t)$ are:

$$\bar{\Phi}_{II}(\omega) = \bar{\Phi}_{22}(\omega) = (B^6\gamma^2/72) \left[\bar{\Phi}_{\xi\xi}(\Omega - \omega) + \bar{\Phi}_{\xi\xi}(\Omega + \omega)\right]$$

(20)

$$\bar{\Phi}_{12}(\omega) = \bar{\Phi}_{21}(-\omega) = (iB^6\gamma^2/72)[\bar{\Phi}_{\xi\xi}(\Omega-\omega) - \bar{\Phi}_{\xi\xi}(\Omega+\omega)]$$

(21)

where $\tilde{\Phi}_{\xi\xi}$ is the spectral density of the nondimensional velocity $\xi(t)$ per unit physical frequency (rad/s). In obtaining Eqs. (20) and (21), the relation $\tilde{\Phi}_{\xi\xi}(\omega) = \tilde{\Phi}_{\eta\eta}$ has been used, since the $\xi(t)$ and $\eta(t)$ processes are identically distributed. Furthermore, if $\xi(t)$ and $\eta(t)$ are wide-band processes with a slowly varying spectral density in the frequency region of interest, then, in that region

$$\bar{\Phi}_{II}(\omega) = \bar{\Phi}_{22}(\omega) \simeq (B^6 \gamma^2/36) \bar{\Phi}_{\xi\xi}$$

and $Z_1(t)$ and $Z_2(t)$ also become nearly uncorrelated.

In the deterministic analysis where the effect of turbulence is not considered, the equation of motion in a hovering flight reduces to one with constant coefficients. Since damping exists in the system, the uncoupled flapping mode is always stable. Therefore, instability can only be caused by the turbulence.

The second-order linear stochastic differential equation of the form, Eq. (17), has been considered by Ariaratnam and Tam.²¹ In order to apply Stratonovich's stochastic averaging method (Appendix A), Eq. (17) must be transformed into two first-order equations. Let

$$\beta = A(\psi)\cos\theta$$
, $\dot{\beta} = -A(\psi)p\sin\theta$, $\theta = p\psi + \nu(\psi)$

^{\$}Stationarity of a random process is interpreted here in the weak sense.

Table 1 Periodic coefficients for coupled flapping-torsional motion

Coefficient	Region	Function form	Coefficient	Region	Function form
C	1 2 3	$B^{4}/4 + B^{3}\mu \bar{S_{1}}/3$ $C_{1} + \mu^{4}(1/16 - \bar{C_{2}}/12 + \bar{C_{4}}/48)$ $-C_{1}$	$C_{lpha \xi}$	1 2 _n 3, 2 _r	$B^{3} \bar{C}_{1}/3 C_{\alpha\xi 1} + \mu^{3} (\bar{S}_{2}/12 - \bar{S}_{4}/24) 0$
C_{η}	1 2 3	$B^{3}\bar{S}_{1}/3 \ C_{\eta l} + \mu^{3}(1/4 - \bar{C}_{2}/3 + \bar{C}_{4}/12) \ - C_{\eta l}$	K_{lpha}	$\begin{array}{c} 1, 2_n \\ 2_r \\ 3 \end{array}$	0 $\mu^{5} (\bar{S}_{1}/48 - \bar{S}_{3}/96 + \bar{S}_{5}/48)$ $-B^{5}/5 - B^{4}\mu \bar{S}_{1}/2 - B^{3}\mu^{2}(1 - \bar{C}_{2})/6$
C_{ξ}	1 2 3	$\begin{array}{l} B^3 \bar{C}_1/3 \\ C_{\xi I} + \mu^3 (\bar{S}_2/6 - \bar{S}_4/12) \\ - C_{\xi I} \end{array}$	$K_{lpha\eta}$	1, 2 _n 2 _r 3	0 $\mu^4 (5\bar{S_1}/48 - 5\bar{S_3}/96 + \bar{S_5}/96)$ $-B^4 \bar{S_1}/2 - B^3 \mu (1 - \bar{C_2})/3$
K	1 2 3	$B^{3} \mu \bar{C}_{1}/3 + B^{2} \mu^{2} \bar{S}_{2}/4$ $K_{1} + \mu^{4} (-\bar{S}_{2}/12 + \bar{S}_{4}/24)$ $-K_{1}$	$K_{\alpha \xi}$	$\begin{array}{c} 1, 2_n \\ 2_r \\ 3 \end{array}$	0 $\mu^4 (\bar{C}_1/48 + \bar{C}_3/48 + \bar{C}_5/16)$ $-B^4 \bar{C}_1/2 - B^3 \mu \bar{S}_2/3$
K_{η}	1 2 3	$B^3 ar{C}_1/3 + B^2 \mu ar{S}_2/2 \ K_{\eta l} + \mu^3 (- ar{S}_2/3 + ar{S}_4/6) \ - K_{\eta l}$	ℓ_{reta}	$\begin{array}{c} 1, 2_n \\ 2_r \\ 3 \end{array}$	0 $\mu^4 (\bar{S}_2/24 - \bar{S}_4/48)$ $B^3 \mu \bar{C}_1/3 + B^2 \mu^2 \bar{S}_2/4$
K_{ξ}	1 2 3	$-B^{3}\bar{S}_{1}/3 + B^{2}\mu\bar{C}_{2}/2 K_{\xi 1} + \mu^{3} (-\bar{C}_{2}/6 + \bar{C}_{4}/6) -K_{\xi 1}$	$\ell_{reta\eta}$	$\begin{array}{c} 1, 2_n \\ 2_r \\ 3 \end{array}$	0 $\mu^{3} (\bar{S}_{2}/6 + \bar{S}_{4}/24)$ $B^{3} \bar{C}_{1}/3 + B^{2} \mu \bar{S}_{2}/2$
m_{lpha}	1 2 3	$B^{5}/5 + B^{4}\mu \bar{S}_{1}/2 + B^{3}\mu^{2}(1 - \bar{C}_{2})/6$ $m_{\alpha l} + \mu^{5}(\bar{S}_{1}/24 - \bar{S}_{3}/48 + \bar{S}_{5}/240)$ $-m_{\alpha l}$	$\ell_{reta\epsilon}$	$\begin{array}{c} 1, 2_n \\ 2_r \\ 3 \end{array}$	0 $\mu^{3} (\bar{C}_{2}/12 - \bar{C}_{4}/12)$ $-B^{3} \bar{S}_{1}/3 + B^{2} \mu \bar{C}_{2}/2$
$m_{lpha\eta}$	1 2 3	$B^{4}\bar{S}_{1}/2 + B^{3}\mu(1 - \bar{C}_{2})/3$ $m_{\alpha\eta 1} + \mu^{4} (5\bar{S}_{1}/24 - 5\bar{S}_{3}/48 + \bar{S}_{5}/48)$ $- m_{\alpha\eta 1}$	$\ell_{r\dot{eta}}$	$\begin{array}{c} 1, 2_n \\ 2_r \\ 3 \end{array}$	0 $\mu^4(-1/32 + \bar{C}_2/24 - \bar{C}_4/96)$ $B^4/4 + B^2\mu\bar{S}_1/3$
$m_{lpha \xi}$	1 2 3	$B^{4}\bar{C}_{1}/2 + B^{3}\mu\bar{S}_{2}/3$ $m_{\alpha\xi 1} + \mu^{4} (\bar{C}_{1}/24 - \bar{C}_{3}/16 - \bar{C}_{5}/48)$ $-m_{\alpha\xi 1}$	$\ell_{r\hat{eta}\eta}$	$\begin{array}{c} 1, 2_n \\ 2_r \\ 3 \end{array}$	0 $\mu^{3}(-1/8 + \bar{C}_{2}/6 - \bar{C}_{4}/24)$ $B^{3}\bar{S}_{1}/3$
C_{lpha}	$ \begin{array}{c} 1\\2_n\\3,2_r \end{array} $	$B^{4}/4 + B^{3} \mu \bar{S}_{1}/3$ $C_{\alpha l} + \mu^{4} (1/32 - \bar{C}_{2}/24 + \bar{C}_{4}/96)$ 0	$\ell_{reta \xi}$	$\begin{array}{c} 1, 2_n \\ 2_r \\ 3 \end{array}$	0 $\mu^{3} (-\bar{S_{2}}/12 + \bar{S_{4}}/24)$ $B^{3}\bar{C_{1}}/3$
$C_{lpha\eta}$	$ \begin{array}{c} 1\\ 2_n\\ 3,2_r \end{array} $	$B^{3}\bar{S}_{1}/3 \\ C_{\alpha\eta l} + \mu^{3} (1/8 - \bar{C}_{2}/6 + \bar{C}_{4}/24) \\ 0$			

Note: $\bar{C}_n = \cos n\psi$, $\bar{S}_n = \sin n\psi$.

Equation (17) may be replaced by two equations for $A(\psi)$ and $\nu(\psi)$:

$$\dot{A} = P(A, \theta, \psi) \sin \theta$$

$$\dot{\nu} = A^{-1} P(A, \theta, \psi) \cos \theta \tag{22}$$

where $P = [-(h+Z_1)\sin\theta + p^{-1}Z_2\cos\theta]A$, and Z_1 , Z_2 are treated as functions of nondimensional time ψ . If the correlation times of Z_1 and Z_2 in the nondimensional time scale are small compared with h, then (A,ν) may be approximated by a vector Markov process. Carrying out both stochastic and time averaging, one obtains a pair of Itô equations:

$$dA = \epsilon m_1 d\psi + \epsilon^{1/2} [\sigma_{II} dW_1 + \sigma_{I2} dW_2]$$

$$d\nu = \epsilon m_2 d\psi + \epsilon^{1/2} [\sigma_{2I} dW_1 + \sigma_{22} dW_2]$$
(23)

where $W_l(\psi)$ and $W_2(\psi)$ are independent Wiener processes, and

$$\epsilon m_1 = -k_1 A = -\left\{ (1/2)h - (\pi/8)\left[2\Phi_{II}(0) + 3\Phi_{II}(2p) + (3/p^2)\Phi_{22}(2p) + (6/p)\Psi_{2I}(2p)\right]\right\}A$$

$$\epsilon m_{2} = -k_{2} = -(\pi/4)[(2/p)\Phi_{2l}(2p) - \Psi_{1l}(2p)$$

$$-(1/p^{2})\Psi_{22}(2p)]$$

$$\epsilon (\sigma\sigma')_{1l} = k_{3}A^{2} = (\pi/4)[2\Phi_{1l}(0) + \Phi_{1l}(2p)$$

$$+(1/p^{2})\Phi_{22}(2p) + (2/p)\Phi_{2l}(2p)]A^{2}$$

$$\epsilon (\sigma\sigma')_{22} = k_{4} = (\pi/4)[\Phi_{1l}(2p) + (2/p^{2})\Phi_{22}(0)$$

$$+(1/p^{2})\Phi_{22}(2p)]$$

$$\epsilon (\sigma\sigma')_{12} = \epsilon (\sigma\sigma')_{2l} = -(\pi/2p)\Phi_{12}(0)A$$
(24)

The Φ_{jk} and Ψ_{jk} are cosine and sine spectral densities and cross-spectral densities of $Z_j(\psi)$ referred to the non-dimensional frequency ω/Ω , defined as:

$$= \begin{cases} (1/\pi) \int_0^\infty E[Z_j(\psi) Z_k(\psi + \chi)] e^{-iu\chi} d\chi & \text{if } j = k \\ \\ (1/2\pi) \int_0^\infty E[Z_j(\psi) Z_k(\psi + \chi)] e^{-iu\chi} d\chi & \text{if } j \neq k \end{cases}$$
 (25)

 $\Phi_{ik}(u) + i\Psi_{ik}(u)$

The conversion from Φ_{jk} , Eqs. (20) and (21), to Φ_{jk} is given by:

$$\bar{\Phi}_{ik}(\omega) = (1/\Omega)\Phi_{ik}(\omega/\Omega) \tag{26}$$

For the special case where $\xi(t)$ and $\eta(t)$ are stationary, uncorrelated, and identically distributed wide-band random processes, the transformation into $Z_I(t)$ and $Z_2(t)$ through Eqs. (18) and (19) preserves these properties. Then all the cross-spectral densities (either cosine or sine) are zero, and all the sine spectral densities are nearly zero. For such a case,

$$(\sigma\sigma')_{12} = (\sigma\sigma')_{21} = 0, \quad m_2 \simeq 0$$

and the two components, A and ν , of the vector Markov process become decoupled. Furthermore, each component is itself a scalar Markov process. Of particular interest is the A-process, since

$$A = (\beta^2 + p^{-2}\dot{\beta}^2)^{1/2}$$

Therefore, boundedness in A implies boundedness in both β and $\dot{\beta}$.

The transition probability density $q_A(a,\psi|a_0,\psi_0)$ satisfies the Fokker-Planck equation (Appendix A):

$$\frac{\partial q_A}{\partial \psi} = k_1 \frac{\partial}{\partial a} (aq_A) + (k_3/2) \frac{\partial^2}{\partial a^2} (a^2 q_A)$$
 (27)

where k_1 and k_3 are now

$$k_I = (I/2)\,h - (\pi/8)\,[2\Phi_{II}(\theta) + 3\Phi_{II}(2p) + 3p^{-2}\Phi_{22}(2p)]$$

$$k_3 = (\pi/4) [2\Phi_{II}(0) + \Phi_{II}(2p) + p^{-2}\Phi_{22}(2p)]$$

The solution of Eq. (27), satisfying also the initial condition $q_A(a, \psi_0 | a_0, \psi_0) = \delta(a - a_0)$ is:

$$q_A = a^{-1} (2\pi k_3 \chi)^{-1/2} \exp\{-[\ln(a/a_0) + k_3 k_5 \chi]^2 / (2k_3 \chi)\}$$
(28)

where $\chi = \psi - \psi_0$, $k_5 = (k_1/k_3) + 1/2$. From Eq. (28), the moments of the response amplitude A are evaluated to be:

$$M_n(\chi) = E[A^n(\psi)] = M_n(\psi_0) \exp\{-n[k_1 - (n-1)(k_3/2)](\psi - \psi_0)\} \quad n = 1, 2, ...$$
(29)

from which the condition for stability in the *n*th moment is:

$$2k_1 - (n-1)k_3 > 0 (30)$$

Letting $h = B^4 \gamma / 8$ and

$$\Phi_{II} = \Phi_{22} = (B^6 \gamma^2 / 36) \Phi_{\xi\xi}$$

the stability condition, Eq. (30), becomes

$$\Phi_{\epsilon\epsilon} < 18\{\pi B^2 \gamma [2(1+p^{-2}) + n(3+p^{-2})]\}^{-1}$$
 (31)

The transition probability density, Eq. (28), represents the most complete solution attainable within the present framework of analysis. The stability condition, Eq. (30), for moments of arbitrary orders is also the most complete. For practical purposes, however, second-moment stability is usually considered adequate. It is, therefore, of interest to examine inequality (31), for the case n=2. The physical parameters on the left-hand side of Eq. (31) for current helicopter blade designs are in the range of $\gamma \sim 7$, $B \sim 1$, $p \sim 1$. Then the second-moment instability can occur only if $\Phi_{\xi\xi}$ is greater than about 0.025.

Concluding Remarks

The turbulence-induced instability for the simple case of uncoupled flapping in a hovering flight is theoretically interesting, since closed-form solutions can be obtained for the transition probability density and the stability conditions for all stochastic moments. Considerable insight can be gained from the analysis. However, the turbulence spectral level of the order of 0.025 on the nondimensional velocity and nondimensional frequency scales, which may cause such an instability, is rather high to be expected of natural turbulence of a geothermal origin, although it may be possible in the wakes of other moving objects. For example, for a 5-m blade rotating at 3-4 rps, this nondimensional level would correspond to about 14 (m/s)²/rad/s in physical units. Therefore, the real threat of turbulence to the rotor blade stability appears to be in coupled motions and in high-speed forward flights, which is discussed in Part II.

The representation of blade loadings using the steady and quasisteady aerodynamics is admittedly a first approximation. The closed-form results obtained for the case of uncoupled flapping in a hovering flight suggest that air loads near twice the blade rotation frequency contribute importantly toward changing the stability condition of the system. However, the trends established in this exploratory study are expected to remain essentially valid if and when the more accurate unsteady aerodynamics are used in future, more refined analyses.

Appendix A: Markov Processes and Approximate Markov Processes

A random process (generally vector-valued) is a Markov process if its future probabilistic structure depends only on the present state and is independent of its past history. A sufficient condition for a random process X(t) to be Markovian is that the increments within arbitrary nonoverlapping time intervals are statistically independent; that is, $X(t_2) - X(t_1)$ and $X(t_4) - X(t_3)$ are independent, provided that $t_1 < t_2 \le t_3 < t_4$.

Among various Markov processes, the diffusive Markov process is governed by an Itô stochastic difference equation of the form (see, for example, Ref. 22):

$$dX_i = \epsilon m_i(X, t) + \epsilon^{1/2} \sigma_{ik}(X, t) dW_k(t)$$
 (A1)

where X_j are components of X(t), $W_k(t)$ are independent unit Wiener (Brownian motion) processes, and the usual summation convention of repeated indices in a product is implied. The coefficients m_j and σ_{jk} are called the drift and diffusion coefficients, respectively. The positive parameters ϵ and $\epsilon^{1/2}$ on the right-hand side of the equation are used to indicate the orders of magnitude for the two terms when both are equally significant.

Each unit Wiener process is itself a Markov process. Furthermore, it is Gaussian distributed with a zero mean, and

$$E\{[W_k(t) - W_k(s)]^2\} = |t - s| \tag{A2}$$

Equation (A2) implies that

$$E\{[dW_k(t)]^2\} = dt$$
 (A3)

The stochastic differential equation, Eq. (A1), is equivalent to the integral equation:

$$X_{j} = X_{j}(t_{0}) + \epsilon \int_{t_{0}}^{t} m_{j}(X, u) du + \epsilon^{1/2} \int_{t_{0}}^{t} \sigma_{jk}(X, u) dW_{k}(u)$$
(A4)

In the sense of Itô, the last integral in Eq. (A4) is interpreted as a forward stochastic integral; i.e.,

$$\int_{t_0}^{t} \sigma_{jk}(X, u) dW_k(u)$$

$$= 1.i.m. \Sigma \sigma_{jk}(X, u) [W_k(u_{\ell+1}) - W_k(u_{\ell})]$$
(A5)

where l.i.m. denotes a mean-square limit.

From Eq. (A1), one can obtain another Itô equation for an arbitrary scalar function $\phi(X)$, provided that ϕ is twice differentiable with respect to the components of X:

$$d\phi = \left[\frac{\partial\phi}{\partial t} + \epsilon \left(m_j \frac{\partial\phi}{\partial X_j} + 1/2\sigma_{jl}\sigma_{kl} \frac{\partial^2\phi}{\partial X_j\partial X_k}\right)\right]dt$$
$$+ \epsilon^{1/2}\sigma_{jk} \frac{\partial\phi}{\partial X_j} dW_k \tag{A6}$$

Equation (A6) is, of course, reducible to Eq. (A1) when $\phi = X_i$.

Relation (A6) is known as Itô's lemma or Itô's differential rule. In particular, letting $\phi = X_r X_c$, one obtains

$$d(X_r X_s) = \epsilon (m_r X_s + m_s X_r + \sigma_{r\ell} \sigma_{s\ell}) dt$$

$$+ \epsilon^{1/2} (\sigma_{rk} X_s + \sigma_{sk} X_r) dW_k$$
(A7)

It is convenient to use the Itô stochastic integral and differential equation when dealing with diffusive Markov processes. The ensemble average of an Itô stochastic integral is zero, as can be deduced from the definition, Eq. (A5). By the same token, the ensemble average of the last term in Eq. (A1) or the last term in Eq. (A6) must also be zero. This simplifies the calculation of the ensemble averages of X_j and $\phi(X)$ since they are governed by the conventional (and deterministic) differential equations:

$$dE[X_i]/dt = \epsilon E[m_i]$$
 (A8)

$$dE[\phi(X)]/dt = E\left[\frac{\partial \phi}{\partial t} + \epsilon \left(m_j \frac{\partial \phi}{\partial X_j} + 1/2\sigma_{jl}\sigma_{kl}\frac{\partial^2 \phi}{\partial X_j\partial X_k}\right)\right]$$
(A9)

In some cases it may be possible to obtain the transition probability density $q(\mathbf{x},t|\mathbf{x}_0,t_0)$ of $\mathbf{x}(t)$, governed by the following parabolic differential equation called the Fokker-Planck (or Kolmogorov forward) equation:

$$\frac{\partial q}{\partial t} + \epsilon \frac{\partial}{\partial x_i} (m_j q) - \frac{\epsilon}{2} \frac{\partial^2}{\partial x_i \partial x_k} (\sigma_{j\ell} \sigma_{k\ell} q) = 0$$
 (A10)

subject to the initial condition:

$$q(\mathbf{x}, t_0 | \mathbf{x}_0, t_0) = \delta(\mathbf{x} - \mathbf{x}_0) \tag{A11}$$

and some suitable boundary conditions. Note that the drift and diffusion coefficients in Eq. (A1) appear again in Eq. (A10), but they are treated here as functions of the deterministic state variables x_j and time t. The transition probability is a conditional probability. If the drift and diffusion coefficients are independent of time, then q tends to the unconditional probability density p(x) of a stationary Markov process as the transition time $t-t_0$ increases. Being independent of time t, the stationary state probability density p is governed by:

$$\frac{\partial}{\partial x_i} (m_i p) - (1/2) \frac{\partial^2}{\partial x_i \partial x_k} (\sigma_{j\ell} \sigma_{k\ell} p) = 0$$
 (A12)

Markov processes in general and the Wiener process in particular are mathematical idealizations. The real interest of an engineer lies in the approximation of real random phenomena by such processes. Obviously, for an approximation to be valid, certain conditions must be satisfied. These will be discussed later.

Let the dynamical law of a physical problem be represented by

$$dX_{i}^{*}/dt = \epsilon f_{i}(X^{*},t) + \epsilon^{1/2}g_{ik}(X^{*},t)\xi_{k}(t)$$
 (A13)

where ξ_k are "physical" random processes. In the sequel, X^* will be referred to as the response and ξ_k as the excitations. It is useful to introduce the following definition of the correlation time of a random process as a suitable measure of memory of the represented random phenomenon:

$$\tau_c = \int_0^\infty \tau |R(\tau)| d\tau / \int_0^\infty |R(\tau)| d\tau$$
 (A14)

where R is the correlation function of the random process and τ is the time difference. It has been assumed tacitly that the process is at least weakly stationary and with a zero mean. If the relaxation time of the response is much longer than the correlation time of every excitation, then the response is expected to be close to a Markov process in some sense. Equation (A13) suggests that the relaxation time of the response X^* is of the order of ϵ^{-1} ; therefore, X^* may be approximated by a Markov process if the correlation times of ξ_k are all much shorter than ϵ^{-1} .

We shall assume that a comparison between the relaxation time of the response and the correlation times of the excitations justifies the substitution of X^* by a Markov process X. The question now remains as to how Eq. (A13) can be converted to an equivalent Itô equation, Eq. (A1). A fundamental difference between these two equations lies in the fact that $\mathrm{d}W_k(t)$ are independent of X(t), whereas $\xi_k(t)$ are correlated with $X^*(t)$. To account for the correlation between the response and the excitations of a physical system at the same time instant t, Stratonovich has proposed a stochastic averaging procedure according to which 23

$$m_{j} = f_{j}(X,t) + \int_{-\infty}^{0} \left[\frac{\partial}{\partial X_{\ell}} g_{jk}(X,t) \right] g_{ir}(X,t+\tau)$$

$$E[\xi_{k}(t)\xi_{r}(t+\tau)] d\tau \tag{A15}$$

$$\sigma_{j\ell}\sigma_{k\ell} = \int_{-\infty}^{\infty} g_{j\tau}(X,t)g_{ks}(X,t+\tau)$$

$$E[\xi_{\tau}(t)\xi_{s}(t+\tau)]d\tau \tag{A16}$$

where distinction between X and X^* has been removed. Equation (A16) gives the elements of the product matrix $\sigma\sigma'$ which are required in the computation of the ensemble average, Eq. (A9), as well as the formulation of the Fokker-Planck equation, Eq. (A10). Matrix σ itself is not needed in practice. Stratonovich further assumes that the parameter ϵ in Eq. (A13) is small to justify taking time averages of Eqs. (A15) and (A16) for further simplification. The entire procedure, proposed initially on pure physical grounds, was later verified rigorously by Khasminskii in a limit theorem. 24

In rotor blade dynamics, especially during high-speed forward flights, an essential feature of the equations of motion is the periodic modulation of the coefficients which arises from the blade rotation. This unique feature would be lost if the coefficients were replaced by their time averages. Therefore, for high-speed forward flights, Eqs. (A15) and (A16) must be retained without time averaging.

In the special case in which ξ_k are "physical" white noise processes; i.e.,

$$E[\xi_{\nu}(t)\xi_{r}(t+\tau)] = 2\pi\Phi_{\nu r}\delta(\tau)$$

Eqs. (A15) and (A16) reduce to

$$m_{j} = f_{j}(X,t) + \pi \Phi_{kr} \frac{\partial}{\partial X_{\ell}} g_{jk}(X,t) g_{\ell r}(X,t)$$
 (A17)

$$\sigma_{j\ell}\sigma_{k\ell} = 2\pi\Phi_{rs}g_{jr}(X,t)g_{ks}(X,t)$$
 (A18)

These are the same results obtained independently by Wong and Zakai using a different approach. ²⁵ The second term on the right-hand side of Eq. (A17) is sometimes called the Wong and Zakai correction.

Appendix B: Correlation Time of Turbulence Field

The method of stochastic averaging is valid only if the correlation time of the excitation is short compared with the relaxation time of the response. It is known that damping in certain types of blade motion is quite high; for example, damping in the uncoupled flapping motion $B^4\gamma/16p$ is of the order of 0.5. Therefore, the relaxation time of the blade motion would appear to be short. However, if we are interested only in the flying conditions which are close to becoming unstable, then the total "effective" damping must be small and the hypothesis of a long relaxation time for the response is not unreasonable.

It now remains to justify the assumption of short correlation time in the turbulence. Two types of turbulence contribute to the excitation of a rotor blade: the natural atmospheric turbulence and the vortex wakes generated by the preceding blades or other objects. Both types of turbulence may be assumed as being statistically stationary in time and, at least, locally homogeneous in space. The second-order statistical properties of a random field can be characterized by the space-time correlation function, which, for a stationary and homogeneous turbulence, is a function of the temporal difference and spatial separation. To appreciate the nature of such a correlation function, consider, for the sake of simplicity, the case of a one-dimensional turbulence. For this case, it is convenient to plot the correlation function in the form of contour lines as depicted in Fig. B1a in which τ is the temporal difference and s the spatial separation measured in a suitable frame of reference. The values of the correlation function have been normalized to have a maximum correlation equal to one. Thus, Fig. B1a is actually a plot of the correlation coefficient function. It is possible to choose suitable scales for τ and s, such that the correlation contours have the appearance of concentric circles when s is referred to

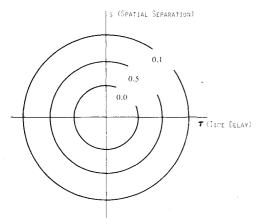


Fig. B1a Correlation contours for one-dimensional turbulence field in a reference frame moving at turbulence convection velocity.

a coordinate system moving at the dominant convection velocity of the turbulence.

The correlation coefficient contours provide a graphical representation of the correlation time and the correlation length, which may, in fact, be defined as the intervals between the intercepts of a representative contour with the τ and s axes. Of course, these measures may change if the turbulence field is viewed from another frame of reference, in particular, from a coordinate system attached to the moving blade.

Let the dominant convection velocity of a one-dimensional turbulence be u and the velocity of the observer be v. Let x_i and x_2 be two coordinate systems moving respectively at velocities u and v. Then referring to a given fixed point in space, we have

$$x = x_2 + vt = x_1 + ut \tag{B1}$$

The spatial separation of two arbitrary points appear differently in the three coordinate systems: $s = x(t_1) - x(t_2)$ in the inertial system, $s_1 = x_1(t_1) - x_1(t_2)$ in the system moving at u, and $s_2 = x_2(t_1) - x_2(t_2)$ in the system moving with the observer. Clearly,

$$s_2 = s - v\tau, \quad s_1 = s - u\tau \tag{B2}$$

where $\tau = t_1 - t_2$. Then,

$$s_2 = s_1 + (u - v)\tau$$
 (B3)

This can be cast in the form

providing a transformation for the correlation contours from the (s_1, τ) space to the (s_2, τ) space. The transformation matrix can be decomposed into

$$\begin{bmatrix} 1 & u-v \\ 0 & 1 \end{bmatrix} = \begin{bmatrix} 1 & 0 \\ 0 & 1 \end{bmatrix} + \begin{bmatrix} 0 & \frac{1}{2}(u-v) & 0 \\ \frac{1}{2}(u-v) & 0 & \frac{1}{2}(u-v) \end{bmatrix}$$

$$+ \begin{bmatrix} 0 & \frac{1}{2}(u-v) & 0 \\ -\frac{1}{2}(u-v) & 0 & \frac{1}{2}(u-v) \end{bmatrix}$$
(B5)
$$(\text{rigid body rotation})$$

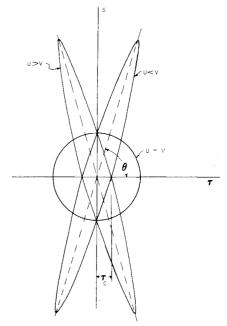


Fig. B1b Stretching of correlation contour due to difference in turbulence convection velocity and reference frame velocity.

The third matrix on the right-hand side of Eq. (B5) accounts for the rotation of the correlation contours, and the second matrix accounts for the change of shape. The area enclosed within each contour should remain the same.

The appearance of the contours in the (s_2, τ) space depends on the difference between u and v. When u = v, the contours are nearly circular. When $u \neq v$, the contours are stretched to an elliptical shape. Figure B1b shows how typical correlation contours may appear for the three cases v = u, v > u, and v < u. The direction in which the contours are stretched is given by the inclination angle:

$$\theta = \tan^{-1}(v - u) \tag{B6}$$

measured counterclockwise from the τ axis. As previously indicated, the intercepts of a typical correlation contour at the τ and s_2 axes are representative of the correlation time and the correlation length. It is interesting to note that the correlation length is always the same for different spatial frames of reference. However, as v becomes much greater than u, the inclination angle θ tends to 90 deg, and the correlation time can become very short. Therefore, the stochastic averaging method is valid when a rotor blade is moving at a speed much greater than the average convection speed of turbulence.

Acknowledgment

This paper is based on work supported by the U.S. Army Research Office under Grant DAAG29-78-G-0039. We also would like to thank the reviewers of this paper for constructive suggestions.

References

¹Shutler, A. G. and Jones, J. P., "The Stability of Rotor Blade Flapping Motion," Aeronautical Research Council R&M No. 3178, May 1958.

²Lowis, O. J., "The Stability of Rotor Blade Flapping Motions at High Tip Speed Ratio," Aeronautical Research Council R&M No. 3544 Jan 1963

³ Wilde, E., Bramwell, A.R.S. and Summerscales, R., "The Flapping Behavior of a Helicopter Rotor at High Tip-Speed Ratio," Aeronautical Research Council CP No. 877, April 1965.

⁴Sissingh, G. J., "Dynamics of Rotors Operating at High Advance Ratios," *Journal of the American Helicopter Society*, Vol. 13, No. 3, July 1968, pp. 56-63.

⁵Peters, D. A. and Hohenemser, K. H., "Application of the Floquet Transition Matrix to the Problems of Lifting Rotor Stability," *Journal of the American Helicopter Society*, Vol. 16, No. 2, May 1971, pp. 25-33.

⁶Hohenemser, K. H. and Yin, S. K., "Some Applications of the Method of Multiblade Coordinates," *Journal of the American Helicopter Society*, Vol. 17, No. 3, July 1972, pp. 3-12.

⁷ Biggers, J. C., "Some Approximations to the Flapping Stability of Helicopter Rotors," NASA SP-352, Feb. 1974, pp. 45-53.

⁸Sissingh, G. J. and Kuczynski, W. A., "Investigations on the Effect of Blade Torsion on the Dynamics of the Flapping Motion," *Journal of the American Helicopter Society*, Vol. 15, No. 2, April 1972, pp. 2-9.

⁹Ormiston, R. A. and Hodges, D. H., "Linear Flap-Lag Dynamics of Hingeless Helicopter Rotor Blades in Hover," *Journal of the American Helicopter Society*, Vol. 17, No. 2, April 1972, pp. 2-14.

¹⁰ Peters, D. A., "Flap-Lag Stability of Helicopter Rotor Blades in Forward Flight," *Journal of the American Helicopter Society*, Vol. 20, No. 4, Oct. 1975, pp. 2-13.

¹¹ Kaza, K.R.V. and Hammond, C. E., "An Investigation of Flap-Lag Stability of Wind Turbine Rotors in the Presence of Velocity Gradients and Helicopter Rotors in Forward Flight," *Proceedings of AIAA/ASME/SAE 17th Structures, Structural Dynamics, Materials Conference*, King of Prussia, Pa., 1976, pp. 421-431.

¹²Goankar, G. H. and Peters, D. A., "Flap-Lag Stability with Dynamic Inflow by the Method of Multi-Blade Coordinates," AIAA Paper 79-0729, 1979.

¹³ Hubolt, J. C. and Brooks, G. W., "Differential Equations of Motion for Combined Flapwise Bending, Chordwise Bending and Torsion of Twisted Nonuniform Rotor Blades," NACA TN 3905, Feb. 1957.

¹⁴Hodges, D. H. and Dowell, E. H., "Nonlinear Equations of Motion for the Elastic Bending and Torsion of Twisted Nonuniform Rotor Blades," NASA TND 7818, Dec. 1974.

¹⁵Hodges, D. H. and Ormiston, R. A., "Stability of Elastic Bending and Torsion of Uniform Cantilever Rotor Blades in Hover with Variable Structural Coupling," NASA TND 8192, April 1976.

¹⁶Hammond, C. E., "An Application of Floquet Theory to Prediction of Mechanical Instability," NASA SP-352, Feb. 1974, pp. 147-158.

¹⁷Gaonkar, G. H. and Hohenemser, K. H., "Stochastic Properties of Turbulence Excited Rotor Blade Vibrations," AIAA Paper 70-548, 1970.

¹⁸Goankar, G. H., Hohenemser, K. H., and Yin, S. K., "Random Gust Response Statistics for Coupled Torsion-Flapping Rotor Blade Vibrations," *Journal of Aircraft*, Vol. 9, Oct. 1972, pp. 726-729.

¹⁹Goankar, G. H., "Random Vibration Peaks in Rotor Craft and the Effects of Nonuniform Gusts," *Journal of Aircraft*, Vol. 14, Jan. 1977, pp. 68-76.

²⁰Wan, F.Y.M., "Nonstationary Response of Linear Time-Varying Dynamical Systems to Random Excitation," ASME Paper 73-APM-6, 1973.

²¹ Ariaratnam, S. T. and Tam, D.S.F., "Random Vibration and Stability of a Linear Parametrically Excited Oscillator," Zeitschrift fuer Angewandte Mathematik und Mechanik, (to appear).

²² Arnold, L., Stochastic Differential Equations: Theory and Applications, John Wiley and Sons, Inc., New York, 1974.

²³ Stratonovich, R. L., *Topics in the Theory of Random Noise*, Vol. II, translated by R. A. Silverman, Gordon and Breach, New York, 1967.

²⁴Khasminskii, R. Z., "A Limit Theorem for the Solution of Differential Equations with Random Right Hand Sides," *Theory of Probability and Applications*, Vol. 11, 1966, pp. 390-405.

²⁵ Wong, E. and Zakai, M., "On the Relation Between Ordinary and Stochastic Equations," *International Journal of Engineering Science*, Vol. 3, No. 2, July 1965, pp. 213-229.